Electronic Supporting Information

Highly efficient iridium(III) phosphors with 2-(4-benzylphenyl)pyridine-type ligand and their high-performance organic light-emitting diodes

Wai-Yeung Wong,*[abcd] Nga-Yuen Chau,[d] Qiwei Wang,[ad] Lu Jiang,[a] Junlong Li[a] and Dongge Ma*[e]

[a] *Antibiotics Research and Reevaluation Key Laboratory of Sichuan Province, Sichuan Industrial Institute of Antibiotics, Chengdu University, Chengdu 610052, P. R. China*

[b] *Department of Applied Biology and Chemical Technology, The Hong Kong Polytechnic University, Hung Hom, Hong Kong, P. R. China. E-mail: wai-yeung.wong@polyu.edu.hk*

[c] *The Hong Kong Polytechnic University Shenzhen Research Institute, Shenzhen 518057, P. R. China*

[d] *Department of Chemistry and Institute of Advanced Materials, Hong Kong Baptist University, Waterloo Road, Kowloon Tong, Hong Kong, P. R. China*

[e] *State Key Laboratory of Luminescent Materials and Devices, Center for Aggregation-Induced Emission, South China University of Technology, Guangzhou 510640, P. R. China. E-mail: msdgma@scut.edu.cn*

Experimental section

General procedures and materials: All reactions were performed under an inert nitrogen atmosphere with the use of a Schlenk line. Glasswares were dried in oven prior to use. Commercially available reagents were used without purification unless otherwise stated. Solvents were purified by distillation over appropriate drying agents. All reactions were monitored by thin-layer chromatography (TLC) with Merck pre-coated aluminum plates. Products were separated and purified by column chromatography with silica gel. Compounds $Ir(acac)_3$, $IrCl_3.3H_2O$, K_2PtCl_4, $Pd(PPh_3)_4$, 4-bromobenzylbromide and other starting materials were commercially available and used as received unless otherwise specifically mentioned. The aryl boronic acid was prepared as reported by the literature method.[1]

Physical measurements: Fast atom bombardment (FAB) mass spectra were recorded on a Finnigan MAT SSQ710 system. Proton and carbon NMR spectra were measured in $CDCl_3$ on a Bruker Ultra-shield 400 MHz spectrometer and tetramethylsilane (TMS) was used as an internal standard for chemical shift calibration. UV/Vis spectra were recorded on a Hewlett Packard 8453 spectrometer. The photoluminescent properties of the compounds were examined using PTI Time Master Model C-720 spectrometer. The photoluminescence quantum yields were investigated in degassed CH_2Cl_2 solution at 298 K against *fac*-[$Ir(ppy)_3$] standard (Φ_p = 0.40). For lifetime measurements, the 337 nm line of a N_2 laser was used as an excitation light source. The data were analyzed by iterative convolution of the luminescence decay profile with the instrument response function using a software package provided by PTI instruments. Electrochemical measurements were conducted

on Potentiostat/Galvanostat/EIS Analyzer model Parstat 4000 at a scan rate of 50 mV s^{-1}. A conventional compartment cell equipped with a carbon glassy working electrode, platinum wire counter electrode and Ag/Ag^{+} reference electrode was used. 0.1 M $[Bu_4N]PF_6$ in THF solution and ferrocene were used as a supporting electrolyte and an internal standard, respectively. The HOMO and LUMO energy levels were determined from the oxidation (E_{ox}) and reduction (E_{red}) potentials using the equations $E_{HOMO} = -(Eox + 4.8)$ eV and $E_{LUMO} = -(E_{red} + 4.8)$ eV which were calculated using the internal standard ferrocene value of -4.8 eV with respect to the vacuum level.[2] Differential scanning calorimetry (DSC) was performed on a Perkin Elmer Pyris Diamond DSC unit under a nitrogen flow at a heating rate of 20 ^{o}C min^{-1} to obtain the glass transition temperature (T_g). The thermal gravimetric analysis (TGA) was conducted on Perkin Elmer TG-6 instrument under nitrogen at the heating rate of 5 ^{o}C min^{-1}.

General procedures for OLED fabrication and measurements: The devices were fabricated by sequentially depositing organic layers under high vacuum thermal evaporation on pre-cleaned indium tin oxide (ITO) glass substrates which were treated with ozone for 10 min. For monochromatic OLEDs manufactured by vacuum deposition, the NPB layer was deposited on a 10 nm MoO_3 thin layer pre-coated on the ITO glass. Then the TCTA layer was placed on the NPB layer. The metallophosphor dopant and host material were co-evaporated to form the emitting layer. TPBi, LiF and Al were evaporated and deposited one by one. All experiments and measurements were performed at room temperature under ambient conditions. The EL spectra and luminance were measured with a PR 650 Spectra Scan spectrometer. The current density-voltage (*L-V*) characteristics of the devices were

recorded using a Keithley 2400/2000 source meter.

Synthesis of cyclometalating ligands L1–L5

Synthesis of L1

The commercially available 4-bromobenzyl bromide (1.12 g, 4.52 mmol) reacted with one equivalent of phenylboronic acid (0.55 g, 4.52 mmol) in the presence of $Pd(PPh_3)_4$ (80 mg) in the solution of toluene (40 mL), ethanol (20 mL) and 2 M Na_2CO_3 (3 mL). A two-necked flask containing 4-benzylphenyl bromide (0.80 g, 3.62 mmol) in dry tetrahydrofuran was cooled in an ice-acetone bath under a nitrogen atmosphere. Then *n*-butyllithium was added to the flask dropwisely followed by trimethylborate and diluted hydrochloric acid. 4-Benzylphenyl boronic acid (0.54 g, 2.53 mmol) was prepared, treated with 2-bromopyridine (0.31 g, 1.95 mmol) through the Suzuki coupling reaction to yield the target compound. The reaction mixture was extracted with ethyl acetate and washed with deionized (D.I.) water. The organic layer was dried over anhydrous Na_2SO_4. The solvent was filtered and then concentrated under vacuum. The mixture was purified by a silica gel column chromatography to afford the white solid product (67%).

Spectral data: MS (MALDI-TOF): *m/z* 245.12 (M^+). ^1H NMR ($CDCl_3$): δ (ppm) 7.80 (d, *J* = 8.0 Hz, 3H, Ar), 7.57–7.53 (m, 6H, Ar), 7.50 (d, *J* = 5.6 Hz, 3H, Ar), 7.10–7.02 (m, 15H, Ar), 6.83 (s, 6H, Ar), 6.63 (d, *J* = 8.4 Hz, 3H, Ar), 3.73–3.70 (m, 6H, CH_2).

Synthesis of L2

A reaction flask was charged with ethanol (20 mL), toluene (40 mL), 4-bromobenzyl bromide (1.18 g, 4.78 mmol) and *p*-tolylboronic acid (0.65 g, 4.78

mmol). The flask was evacuated and filled with nitrogen and then 2 M solution of Na_2CO_3 (3 mL) and $Pd(PPh_3)_4$ (80 mg) were added. The reaction mixture was stirred at 80 ^oC for 15 h. 1-Bromo-4-(4-methylbenzyl)benzene was then purified and then converted to its boronic acid derivative. A mixture of 4-(4-methylbenzyl)phenylboronic acid (0.61 g, 2.68 mmol) and 2-bromopyridine (0.32 g, 2.06 mmol) and tetrahydrofuran was charged with nitrogen, after which a catalytic amount of $Pd(PPh_3)_4$ was added. The mixture was stirred for two days at 110 ^oC. After cooling to room temperature, the mixture was washed with D.I. water and extracted with ethyl acetate. The combined organic layer was dried by Na_2SO_4, filtered and concentrated. After purification by a silica gel column chromatography with a mixture of hexane:CH_2Cl_2 (5:1 v/v), the targeted compound was obtained as a white powder (72%).

Spectral data: MS (MALDI-TOF): *m/z* 259.14 (M^+). ^1H NMR ($CDCl_3$): δ (ppm) 8.67–8.66 (m, 1H, Ar), 7.90 (d, *J* = 8.4 Hz, 2H, Ar), 7.75–7.68 (m, 2H, Ar), 7.29 (d, *J* = 8.4 Hz, 2H, Ar), 7.22–7.19 (m, 1H, Ar), 7.10 (s, 4H, Ar), 4.00 (s, 2H, CH_2), 2.32 (s, 3H, CH_3).

Synthesis of L3

This compound was obtained using the same methodology as described in **L1** but 4-benzylphenylboronic acid (1.20 g, 5.66 mmol) and 2-chloro-4-methylpyridine (0.55 g, 4.35 mmol) were used instead. The 4-methyl-2-(4-benzylphenyl)pyridine was purified by silica gel chromatography eluting with a mixture of hexane:CH_2Cl_2 (3:1, v/v) as a pale yellow oil (66%).

Spectral data: MS (MALDI-TOF): *m/z* 259.14 (M^+). ^1H NMR ($CDCl_3$): δ (ppm) 8.52 (d, *J* = 5.6 Hz, 1H, Ar), 7.89 (d, *J* = 8.4 Hz, 2H, Ar), 7.51 (s, 1H, Ar), 7.30–7.28

(m, 4H, Ar), 7.22–7.20 (m, 3H, Ar), 7.04 (d, J = 5.6 Hz, 1H, Ar), 4.04 (s, 2H, CH_2), 2.40 (s, 3H, CH_3).

Synthesis of L4

This compound was obtained using the same methodology as described in **L1** but 4-benzylphenylboronic acid (1.10 g, 5.19 mmol) and 2-chloro-5-methylpyridine (0.51 g, 3.99 mmol) were used instead. The 5-methyl-2-(4-benzylphenyl)pyridine was purified by silica gel chromatography eluting with a mixture of hexane:CH_2Cl_2 (3:1, v/v) as a white powder (76%).

Spectral data: MS (MALDI-TOF): *m/z* 259.14 (M^+). ^{1}H NMR ($CDCl_3$): δ (ppm) 8.49 (s, 1H, Ar), 7.88 (d, J = 8.4 Hz, 2H, Ar), 7.69 (d, J = 8.0 Hz, 1H, Ar), 7.53 (d, J = 10.4 Hz, 1H, Ar), 7.31–7.25 (m, 4H, Ar), 7.20 (d, J = 6.8 Hz, 3H, Ar), 4.03 (s, 2H, CH_2), 2.36 (s, 3H, CH_3).

Synthesis of L5

This compound was obtained using the same methodology as described in **L1** but 2-chloro-5-trifluoromethylpyridine (0.79 g, 4.35 mmol) and 4-benzylphenylboronic acid (1.20 g, 5.66 mmol) were used instead. 5-Trifluoromethyl-2-(4-benzylphenyl)pyridine was purified by silica gel chromatography eluting with a mixture of hexane:CH_2Cl_2 (2:1, v/v) as a white powder (64%).

Spectral data: MS (MALDI-TOF): *m/z* 313.11 (M^+). ^{1}H NMR ($CDCl_3$): δ (ppm) 8.95 (s, 1H, Ar), 8.08 (d, J = 12.4 Hz, 2H, Ar), 7.94 (d, J = 2.0 Hz, 1H, Ar), 7.81 (d, J = 8.0 Hz, 1H, Ar), 7.37–7.32 (m, 4H, Ar), 7.32–7.24 (m, 3H, Ar), 4.08 (s, 2H, CH_2).

Table S1. Electronic excitation energies (eV) and corresponding oscillator strengths (*f*), main configurations and CI coefficients of the low-lying electronic excited states of the complex **1** calculated by TDDFT//B3LYP/GENECP based on the DFT//B3LYP/ GENECP optimized ground state geometries

	Electronic transition	**Energy [eV/nm][a]**	***f*[b]**	**Composition[c]**	**CI[d]**
Singlet	$S_0 \rightarrow S_1$	2.76/449	0.0222	H→L	0.63235
	$S_0 \rightarrow S_5$	3.17/391	0.0279	H-1→L+1	0.65534
				H-1→L	0.21324
	$S_0 \rightarrow S_{10}$	3.51/354	0.0268	H-2→L	0.57317
	$S_0 \rightarrow S_{13}$	3.64/340	0.0537	H-2→L+2	0.19555
	$S_0 \rightarrow S_{22}$	4.00/310	0.0464	H-4→L+3	0.23097
	$S_0 \rightarrow S_{24}$	4.05/306	0.0830	H-4→L+2	0.40936
				H-2→L+2	0.19317
	$S_0 \rightarrow S_{27}$	4.1762/297	0.0824	H-6→L+1	0.37976

[a] Only the selected low-lying excited states are presented. [b] Oscillator strengths. [c] Only the main configurations are presented. [d] The CI coefficients are in absolute values.

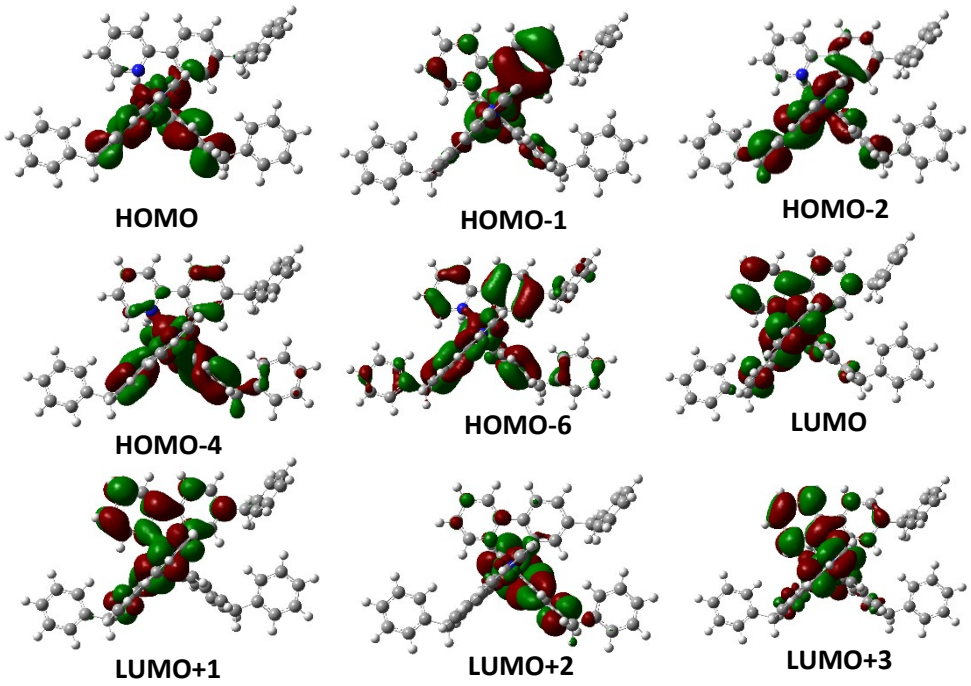

Fig. S1 Electron density maps of the frontier molecular orbital of the complex **1** based on ground state optimized geometry by the DFT calculations at the B3LYP/GENECP level with Gaussian 09W.

Table S2. Electronic excitation energies (eV) and corresponding oscillator strengths (*f*), main configurations and CI coefficients of the low-lying electronic excited states of the complex **2** calculated by TDDFT//B3LYP/GENECP based on the DFT//B3LYP/ GENECP optimized ground state geometries

	Electronic transition	**Energy [eV/nm][a]**	***f*[b]**	**Composition[c]**	**CI[d]**
Singlet	$S_0 \rightarrow S_1$	2.76/449	0.0224	H→L	0.62347
	$S_0 \rightarrow S_3$	2.93/424	0.0165	H→L+2	0.68206
	$S_0 \rightarrow S_7$	3.37/368	0.0287	H-1→L+2	0.54180
	$S_0 \rightarrow S_{13}$	3.64/341	0.0551	H-3→L	0.50437
				H-4→L	0.30676
	$S_0 \rightarrow S_{24}$	4.03/307	0.0889	H-4→L+2	0.38142
				H-3→L+3	0.12600
	$S_0 \rightarrow S_{27}$	4.16/298	0.1237	H-6→L+1	0.34567
				H-6→L	0.31726

[a] Only the selected low-lying excited states are presented. [b] Oscillator strengths. [c] Only the main configurations are presented. [d] The CI coefficients are in absolute values.

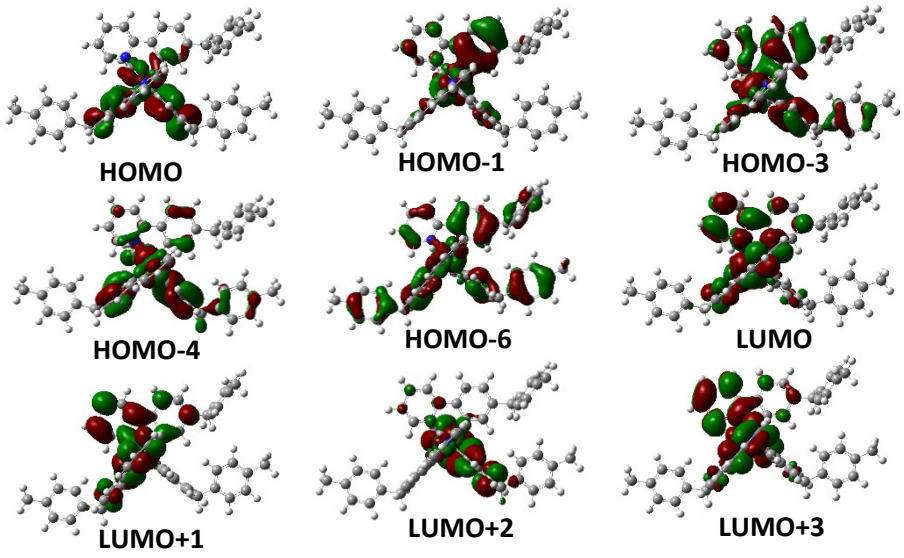

Fig. S2 Electron density maps of the frontier molecular orbital of the complex **2** based on ground state optimized geometry by the DFT calculations at the B3LYP/GENECP level with Gaussian 09W.

Table S3. Electronic excitation energies (eV) and corresponding oscillator strengths (*f*), main configurations and CI coefficients of the low-lying electronic excited states of the complex **3** calculated by TDDFT//B3LYP/GENECP based on the DFT//B3LYP/ GENECP optimized ground state geometries

	Electronic transition	**Energy [eV/nm][a]**	***f*[b]**	**Composition[c]**	**CI[d]**
Singlet	$S_0 \rightarrow S_1$	2.83/438	0.0268	H→L	0.66255
	$S_0 \rightarrow S_3$	2.96/418	0.0155	H→L+2	0.68284
	$S_0 \rightarrow S_4$	3.18/390	0.0351	H-1→L	0.68407
	$S_0 \rightarrow S_{13}$	3.66/338	0.0399	H-3→L	0.48312
				H-2→L+2	0.26565
	$S_0 \rightarrow S_{18}$	3.84/322	0.0559	H-3→L+2	0.44683
				H-2→L+2	0.31953
	$S_0 \rightarrow S_{23}$	4.07/304	0.0620	H-4→L+2	0.45614
	$S_0 \rightarrow S_{27}$	4.21/295	0.0740	H-6→L+1	0.32614

[a] Only the selected low-lying excited states are presented. [b] Oscillator strengths. [c] Only the main configurations are presented. [d] The CI coefficients are in absolute values.

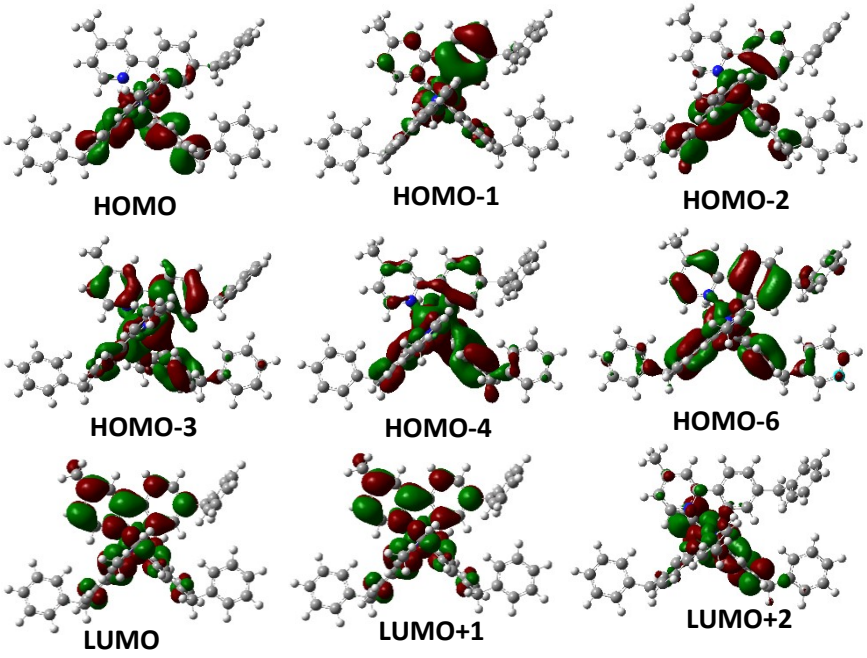

Fig. S3 Electron density maps of the frontier molecular orbital of the complex **3** Based on ground state optimized geometry by the DFT calculations at the B3LYP/GENECP level with Gaussian 09W.

Table S4. Electronic excitation energies (eV) and corresponding oscillator strengths (*f*), main configurations and CI coefficients of the low-lying electronic excited states of the complex **4** calculated by TDDFT//B3LYP/GENECP based on the DFT//B3LYP/ GENECP optimized ground state geometries

	Electronic transition	**Energy [eV/nm][a]**	***f*[b]**	**Composition[c]**	**CI[d]**
Singlet	$S_0 \rightarrow S_1$	2.76/449	0.0213	H→L	0.59737
				H→L+1	0.36140
	$S_0 \rightarrow S_3$	2.92/424	0.0176	H→L+2	0.68345
	$S_0 \rightarrow S_9$	3.43/362	0.0559	H-1→L+2	0.46236
	$S_0 \rightarrow S_{13}$	3.63/343	0.0485	H-3→L	0.51084
	$S_0 \rightarrow S_{24}$	4.01/309	0.0904	H-3→L+2	0.34895
	$S_0 \rightarrow S_{27}$	4.13/300	0.0616	H-6→L+1	0.37768
				H-2→L+5	0.27070

[a] Only the selected low-lying excited states are presented. [b] Oscillator strengths. [c] Only the main configurations are presented. [d] The CI coefficients are in absolute values.

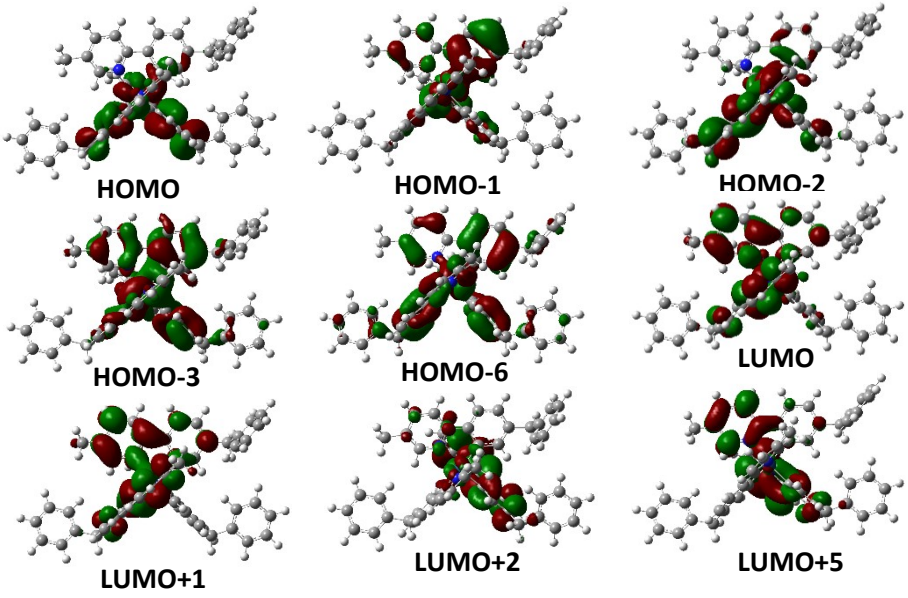

Fig. S4 Electron density maps of the frontier molecular orbital of the complex **4** based on ground state optimized geometry by the DFT calculations at the B3LYP/GENECP level with Gaussian 09W.

Table S5. Electronic excitation energies (eV) and corresponding oscillator strengths (*f*), main configurations and CI coefficients of the low-lying electronic excited states of the complex **5** calculated by TDDFT//B3LYP/GENECP based on the DFT//B3LYP/ GENECP optimized ground state geometries

	Electronic transition	**Energy [eV/nm][a]**	***f*[b]**	**Composition[c]**	**CI[d]**
Singlet	$S_0 \rightarrow S_1$	2.88/430	0.0076	H→L	0.68331
	$S_0 \rightarrow S_3$	3.14/394	0.0182	H-2→L	0.68935
	$S_0 \rightarrow S_9$	3.60/344	0.0395	H-3→L	0.46776
				H→L+4	0.42172
	$S_0 \rightarrow S_{16}$	3.93/316	0.0308	H-2→L+2	0.39441
	$S_0 \rightarrow S_{18}$	3.96/313	0.0822	H-4→L+1	0.54593
	$S_0 \rightarrow S_{27}$	4.28/289	0.2253	H-6→L+1	0.51292
				H-3→L+2	0.23942

[a] Only the selected low-lying excited states are presented. [b] Oscillator strengths. [c] Only the main configurations are presented. [d] The CI coefficients are in absolute values.

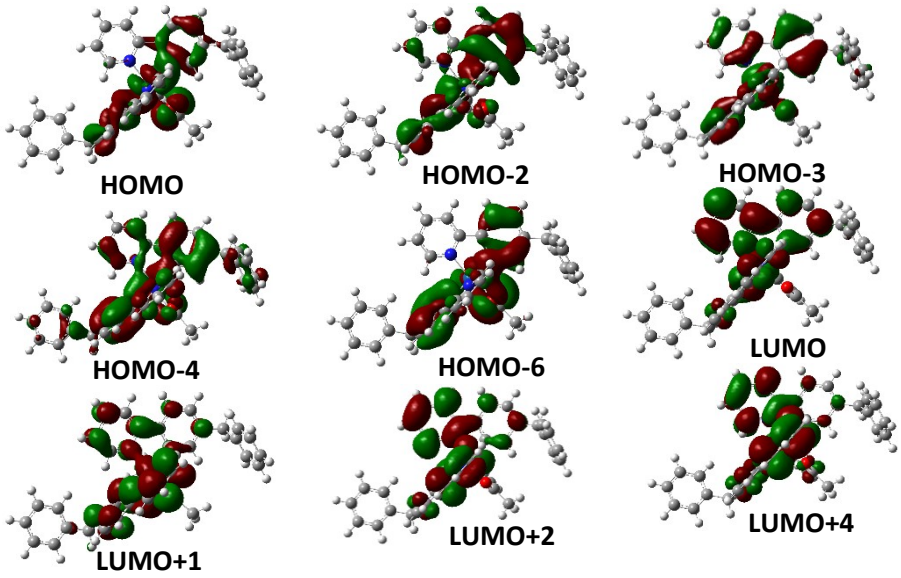

Fig. S5 Electron density maps of the frontier molecular orbital of the complex **5** based on ground state optimized geometry by the DFT calculations at the B3LYP/GENECP level with Gaussian 09W.

Table S6. Electronic excitation energies (eV) and corresponding oscillator strengths (*f*), main configurations and CI coefficients of the low-lying electronic excited states of the complex **6** calculated by TDDFT//B3LYP/GENECP based on the DFT//B3LYP/ GENECP optimized ground state geometries

	Electronic transition	**Energy [eV/nm][a]**	***f*[b]**	**Composition[c]**	**CI[d]**
Singlet	$S_0 \rightarrow S_1$	2.89/429	0.0072	H→L	0.68400
	$S_0 \rightarrow S_3$	3.15/393	0.0215	H-1→L	0.68910
	$S_0 \rightarrow S_9$	3.61/344	0.0363	H→L+4	0.46524
	$S_0 \rightarrow S_{18}$	3.95/314	0.0928	H-4→L+2	0.56995
	$S_0 \rightarrow S_{20}$	4.01/309	0.0334	H-5→L	0.46970
	$S_0 \rightarrow S_{27}$	4.27/291	0.1741	H-6→L+1	0.56997

[a] Only the selected low-lying excited states are presented. [b] Oscillator strengths. [c] Only the main configurations are presented. [d] The CI coefficients are in absolute values.

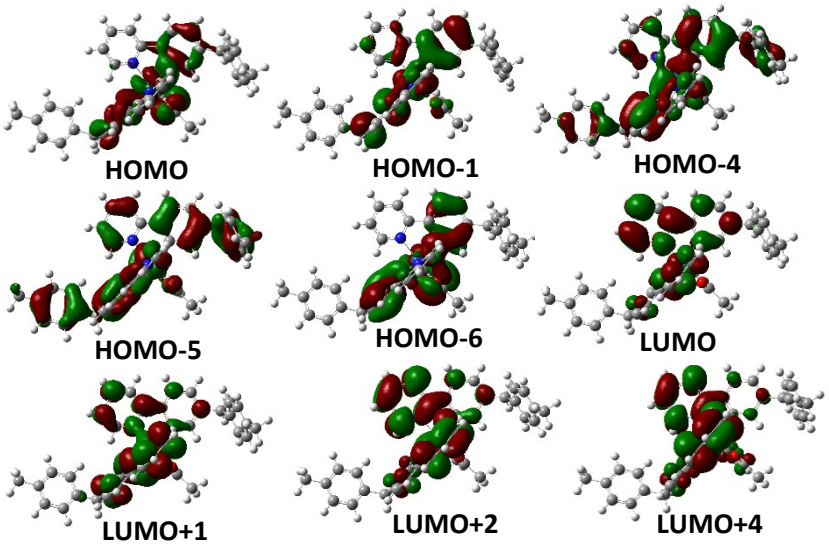

Fig. S6 Electron density maps of the frontier molecular orbital of the complex **6** based on ground state optimized geometry by the DFT calculations at the B3LYP/GENECP level with Gaussian 09W.

Table S7. Electronic excitation energies (eV) and corresponding oscillator strengths (*f*), main configurations and CI coefficients of the low-lying electronic excited states of the complex **7** calculated by TDDFT//B3LYP/GENECP based on the DFT//B3LYP/ GENECP optimized ground state geometries

	Electronic transition	**Energy [eV/nm][a]**	***f*[b]**	**Composition[c]**	**CI[d]**
Singlet	$S_0 \rightarrow S_1$	2.90/427	0.0088	H→L	0.68068
	$S_0 \rightarrow S_3$	3.17/392	0.0209	H-1→L	0.68903
	$S_0 \rightarrow S_9$	3.61/343	0.0781	H-2→L	0.63745
	$S_0 \rightarrow S_{19}$	4.00/310	0.0524	H-4→L+1	0.39485
				H-2→L+2	0.28300
	$S_0 \rightarrow S_{23}$	4.17/297	0.0463	H-5→L+1	0.55766
	$S_0 \rightarrow S_{27}$	4.30/288	0.2523	H-3→L+2	0.24657
				H-5→L	0.22219

[a] Only the selected low-lying excited states are presented. [b]Oscillator strengths. [c]Only the main configurations are presented. [d] The CI coefficients are in absolute values.

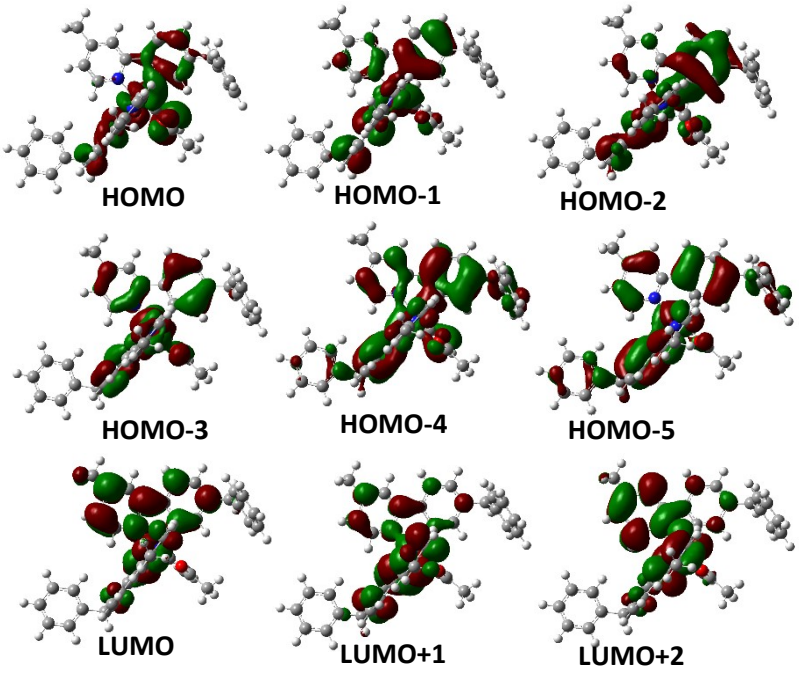

Fig. S7 Electron density maps of the frontier molecular orbital of the complex **7** based on ground state optimized geometry by the DFT calculations at the B3LYP/GENECP level with Gaussian 09W.

Table S8. Electronic excitation energies (eV) and corresponding oscillator strengths (*f*) main configurations and CI coefficients of the low-lying electronic excited states of the complex **8** calculated by TDDFT//B3LYP/GENECP based on the DFT//B3LYP/ GENECP optimized ground state geometries

	Electronic transition	**Energy [eV/nm][a]**	***f*[b]**	**Composition[c]**	**CI[d]**
Singlet	$S_0 \rightarrow S_1$	2.88/431	0.0079	H→L	0.68835
	$S_0 \rightarrow S_3$	3.15/393	0.0216	H-1→L	0.68890
	$S_0 \rightarrow S_9$	3.61/343	0.0641	H-3→L	0.60544
	$S_0 \rightarrow S_{17}$	3.96/313	0.0364	H-2→L+2	0.33306
	$S_0 \rightarrow S_{20}$	4.03/308	0.0772	H-5→L	0.45695
	$S_0 \rightarrow S_{27}$	4.29/289	0.1994	H-6→L+1	0.54541
				H-3→L+2	0.23368

[a] Only the selected low-lying excited states are presented. [b] Oscillator strengths. [c] Only the main configurations are presented. [d] The CI coefficients are in absolute values.

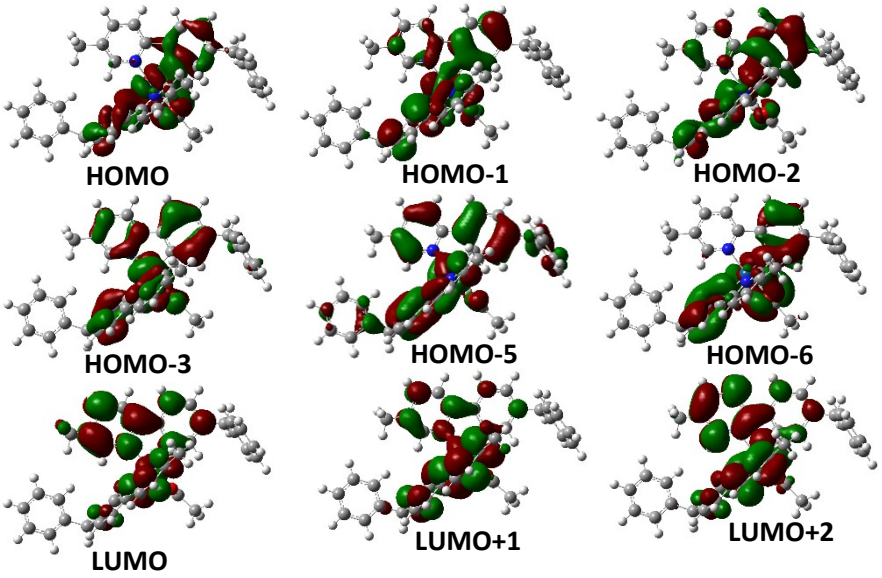

Fig. S8 Electron density maps of the frontier molecular orbital of the complex **8** based on ground state optimized geometry by the DFT calculations at the B3LYP/GENECP level with Gaussian 09W.

Table S9. Electronic excitation energies (eV) and corresponding oscillator strengths (*f*), main configurations and CI coefficients of the low-lying electronic excited states of the complex **9** calculated by TDDFT//B3LYP/GENECP based on the DFT//B3LYP/ GENECP optimized ground state geometries

	Electronic transition	**Energy [eV/nm][a]**	***f*[b]**	**Composition[c]**	**CI[d]**
Singlet	$S_0 \rightarrow S_1$	2.63/471	0.0066	H→L	0.70106
	$S_0 \rightarrow S_3$	3.01/412	0.0267	H-1→L	0.69151
	$S_0 \rightarrow S_{10}$	3.45/360	0.0761	H-3→L	0.60845
				H-1→L+2	0.20766
	$S_0 \rightarrow S_{16}$	3.77/329	0.0781	H-4→L+1	0.58668
				H-3→L+2	0.20620
	$S_0 \rightarrow S_{23}$	4.00/310	0.0711	H-6→L+1	0.39779
				H-5→L	0.26333
	$S_0 \rightarrow S_{28}$	4.14/300	0.0117	H-4→L+2	0.44028

[a] Only the selected low-lying excited states are presented. [b] Oscillator strengths. [c] Only the main configurations are presented. [d] The CI coefficients are in absolute values.

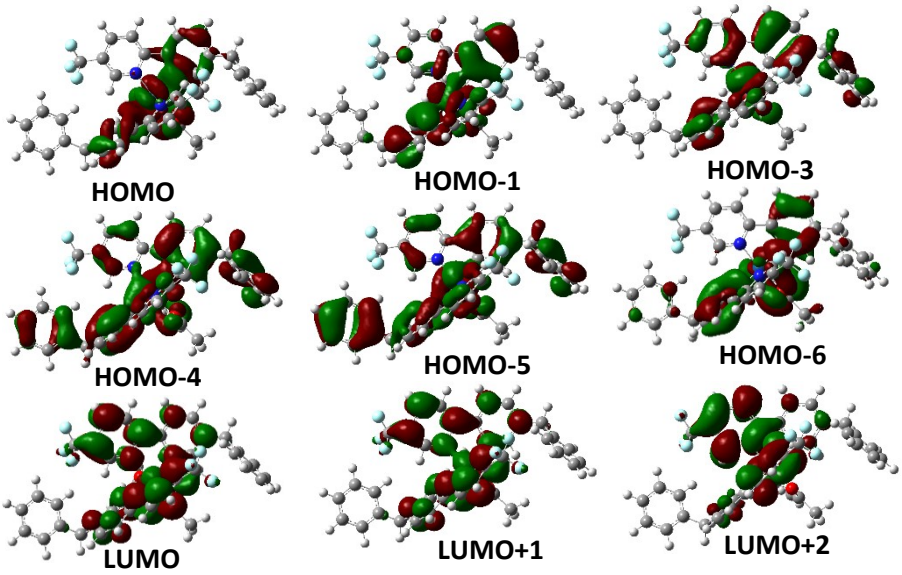

Fig. S9 Electron density maps of the frontier molecular orbital of the complex **9** based on ground state optimized geometry by the DFT calculations at the B3LYP/GENECP level with Gaussian 09W.

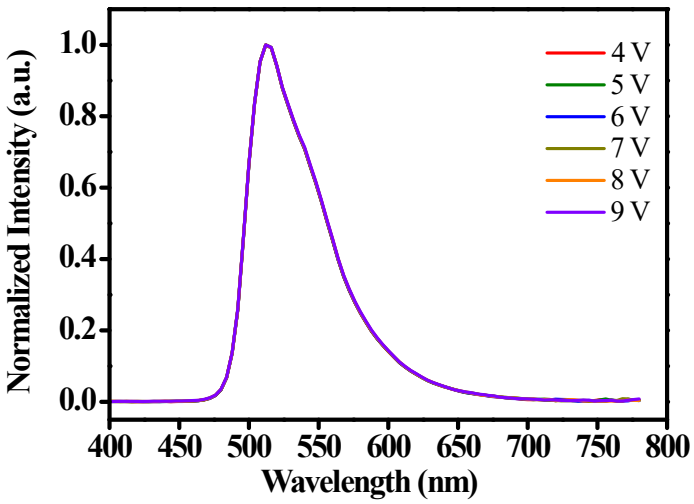

Fig. S10 Voltage independent EL spectra of **4**.

References:

1. S. J. Liu, Q. Zhao, Q. L. Fan and W. Huang, *Eur. J. Inorg. Chem.*, 2008, **13**, 2177.
2. R. S. Ashraf, M. Shahid, E. Klemm, M. Al-Ibrahim, S. Sensfuss, *Macromol. Rapid. Commun.*, 2006, **27**, 1454.